Measurement of miniband parameters of a doped superlattice by photoluminescence in high magnetic fields

R.F. Oliveira, A.B. Henriques, T.E. Lamas, A.A. Quivy,
Instituto de Física, Universidade de São Paulo
Caixa Postal 66318, 05315-970 São Paulo, Brazil

E. Abramof
LAS-INPE, Av. dos Astronautas, 1758 - Jd. Granja,
12227-010, São José dos Campos, Brazil

Abstract

We have studied a 50/50Å superlattice of $GaAs/Al_{0.21}Ga_{0.79}As$ composition, modulation-doped with Si, to produce $n = 1.4 \times 10^{12}$ cm^{-2} electrons per superlattice period. The modulation-doping was tailored to avoid the formation of Tamm states, and photoluminescence due to interband transitions from extended superlattice states was detected. By studying the effects of a quantizing magnetic field on the superlattice photoluminescence, the miniband energy width, the reduced effective mass of the electron-hole pair, and the band gap renormalization could be deduced.

I. INTRODUCTION

The direct measurement of characteristic parameters of low dimensional semiconductor systems, from their optical spectra, requires an experimental technique sensitive enough to detect the singularities in the electronic density of states [1-4]. In superlattices, optical detection of the van Hove singularities associated with electronic minibands has been accomplished by measuring the absorption spectrum due to intraband transitions, in the far infrared wavelength range[1]. Interband optical methods, however, could not be used successfully to provide a direct measurement of the miniband width, due to the formation of saddle point excitons at the edges of the van-Hove singularities[2], with a binding energy which is larger for the M_1 exciton than for the M_0 exciton, due to a negative electronic effective mass along the growth direction in the former case[3]. In heavily doped superlattices, exciton formation is suppressed, due to Coulomb screening and phase-space filling. With sufficient doping, the Fermi level will lay above the energy at top of the electronic miniband, and luminescence from miniband states below the Fermi level should be observed. One drawback, however, is that often the PL of doped superlattices is completely dominated by transitions between localized Tamm states, precluding the detection of interband transitions associated with extended miniband states[4]. When the doping atoms are located in the inner barrier layers of the superlattice, the spatial separation between the electronic charge and the ionized donors gives rise to a strong bending of the band-edges at the boundaries of the superlattice, which causes a shift of the outer wells from resonance with the inner ones, and Tamm states are formed (for a survey on Tamm states in superlattices see Ref.[5]).

If the modulation-doping profile is tailored in order to avoid the formation of Tamm states, then it should be possible to detect the miniband singularities by using interband photoluminescence (PL) spectroscopy. By solving the Schroedinger and Poisson equations, we found the formation of Tamm states is avoided if, in addition to the inner barriers, doping atoms are also added to the outer layers of the superlattice, with an areal concentration about half the value used for the inner ones. In this work we report an investigation of a superlattice sample with such a doping profile, grown by molecular beam epitaxy, by photoluminescence in high magnetic fields. Experiments showed that when the doping level is such that the miniband is fully populated, i.e. the Fermi level lies above the M_1 singularity, luminescence between Landau levels of the M_0 and M_1 valence and conduction band states

can be detected. The miniband parameters can be obtained directly from the oscillations of the photoluminescence intensity as a function of magnetic field, which is described by a doublet of frequencies. By measuring the oscillation frequencies as a function of the photon energy, we can estimate the miniband energy width, the electron-hole pair reduced mass for in-plane movement, and the effective superlattice band gap. The superlattice band gap is lowered by the self-energy correction, arising from the electron exchange interaction, by an amount equal to the so-called band gap renormalization[6] (BGR); For a superlattice with 1.42×10^{12} cm^{-2} electrons per period, our results show that the band gap is lowered by 23.4 meV. This value is intermediate between the band gap renormalization of 52 meV and 21 meV, estimated for a strictly two-dimensional or three-dimensional electron gas of equivalent density, respectively.

II. EXPERIMENTAL

The superlattice sample was grown by molecular beam epitaxy (MBE) and consisted of 20 GaAs quantum wells of 50 Å thickness, separated by 19 $Al_{0.21}Ga_{0.79}As$ inner barriers of thickness 50 Å. Measurement of low-angle X-ray reflectivity measurements confirmed the thickness of the layers. The internal AlGaAs barriers were delta-doped with Si at their center, with an areal density of 1.5×10^{12} cm^{-2}. The outer AlGaAs layers were delta-doped with half of the same areal concentration, at a distance of 25 Å from the adjacent GaAs layer. Shubnikov-de Haas (SdH) measurements of in-plane conductivity were made on approximately square samples, with contacts in the corners, using currents of 200-400 μA. PL measurements were done in the Faraday geometry, using optical fibers and in situ miniature focusing optics. All measurements were done at 2K.

III. RESULTS AND DISCUSSION

Figure 1 shows the Fourier transform of the SdH oscillations for the superlattice sample, for a magnetic field applied normal to the surface of the sample. Two peaks are observed, at $f_{SdH}(M_1) = 23.4$ T and $f_{SdH}(M_0) = 34.9$ T. These peaks are associated with the 'belly' and 'neck' extremal orbits in the mini-Fermi surface[7], and can be labeled by the corresponding saddle points in the density of states, M_0 and M_1. To demonstrate this association, SdH

measurements were done for a magnetic field direction tilted away from the normal to the surface of the sample. In tilted fields, the two peaks show a characteristic behaviour of quasi-three dimensional electrons, whereby the M_0 and M_1 peaks cross over[8,9], as shown in Figure 2. According to Onsager's quasiclassical quantization formula, the Fourier frequencies in the SdH oscillations will be given by $f_{SdH} = \frac{h}{2\ e} A_e$, where A_e are the extremal sections of the mini-Fermi surface, hence for a parabolic electronic in-plane dispersion we obtain

$$f_{SdH}(M_0) = \frac{m_e\ _e}{he}; \quad f_{SdH}(M_1) = \frac{m_e(\ _e \quad _e)}{he}; \tag{1}$$

where m_e is the electronic in-plane effective mass, $_e$ is the Fermi energy, and $_e$ is the energy width of the miniband. The full and dashed lines shown in Figure 2 are the theoretical M_0 and M_1 SdH frequencies, respectively, obtained from equation (1), by solving self-consistently the Schroedinger and Poisson equations, for an infinite $Al_{0.21}Ga_{0.79}As/GaAs$ superlattice, with all GaAs and $Al_{0.21}Ga_{0.79}As$ layers being of width 50A, and doped in the middle of the internal barriers with $N_d = 1.42 \quad 10^{12}\ cm^{\ 2}$. The good agreement between theoretical and experimental Fourier frequencies demonstrates the presence of electrons confined by a superlattice potential, in close agreement with the design parameters.

The electronic effective mass, m_e, was estimated from the temperature dependence of the amplitude of the SdH oscillations, giving $m_e = 0.068 m_0$. Using the experimental values, $m_e = 0.068 m_0$, $f_{SdH}(M_1) = 23.4$ T and $f_{SdH}(M_2) = 34.9$ T, equation (1) gives $_e = 19.6$ meV and $_e = 59.4$ meV.

Figure 3 shows the photoluminescence (PL) spectrum at T = 2 K for the superlattice. A broad emission band is seen above the GaAs gap, which is associated with recombinations between electrons and holes confined by the superlattice potential. The effective superlattice band gap, E_0, the energy corresponding to $E_0 + \ _e$, and the energy corresponding to $E_0 + \ _e$, are shown in Figure 3; these energies were estimated from the analysis below.

In order to demonstrate that the wide PL emission band shown in Figure 3 arises from electron-hole recombinations by charge carriers confined by the superlattice potential, the PL spectra were studied as a function of the applied magnetic field. Figure 4 shows the PL intensity oscillations at fixed photon energies. The oscillations in the PL intensity, at a given photon energy h , will be proportional to[10]

$$I(h\ ;B) \quad \sum_{N,N^0;k_e;k_h} \quad |h\ _h(N^0;k_h)|\ _e(N;k_e)i|^2$$

$$E_0 + \quad N + \frac{1}{2} \quad h!_e + E_e(k_e) + \quad N^0 + \frac{1}{2} \quad h!_h + E_h(k_h) \quad h \tag{2}$$

where the summation is over electronic states, $(N;k_e)$, that are situated below the Fermi level, and over hole states, $(N^0;k_h)$, that contain photoexcited holes. Due to momentum conservation[11,12], transitions occur only if $N^0 = N$ and $k_h = k_e = k$, and we obtain

$$I(h \;;B) \quad jh_h j_e ij^2 \sum_{N;k} \left[E_0 + \quad N + \frac{1}{2} \frac{heB}{} + E_e(k) + E_h(k) \quad h \right] \tag{3}$$

where $_e$, $_h$ are the electron and hole superlattice envelope wave functions, and is the reduced mass of the electron-hole pair. In the tight-binding approximation the electronic and hole miniband dispersion will be given by,

$$E_e(k) = \frac{_e}{2}(1 \quad \cos kd); \qquad E_h(k) = \frac{_h}{2}(1 \quad \cos kd); \tag{4}$$

where d is the period of the superlattice, and by following the steps described in[13], from equations (3,4) we can obtain an analytical expression for the PL intensity oscillations:

$$I(h \;;B) \quad \exp \quad \frac{2}{heB} \quad J_0 \left(\frac{_e + \quad _h}{heB =} \right) \cos \; 2 \left(\frac{h \quad E_0 \quad \frac{_e + \quad _h}{2}}{heB =} \right) \tag{5}$$

where is an energy level broadening parameter. Equation (5) yields a doublet of frequencies of oscillation, associated with saddle points M_0 and M_1, whose values are

$$f_{PL}(M_0) = \frac{h \quad E_0}{he}; \qquad f_{PL}(M_1) = \frac{h \quad E_0 \quad _e \quad _h}{he} \tag{6}$$

Figure 5 shows the oscillations in the PL intensity as a function of magnetic eld for a photon energy of $h \;\; = 1{:}6199$ eV, and a theoretical t to equation (5), including a monotonous parabolic background. The tting procedure yields the values for $f_{PL}(M_0) = 22{:}2$ T, and $f_{PL}(M_1) = 8{:}0$ T.

The tting procedure was repeated for all photon energies measured. Figure 6 shows the frequencies of oscillations of the PL intensity in a magnetic eld as a function of the photon energy. A linear dependence of the PL oscillation frequencies on the photon energy is obtained, in agreement with eq.(6).

The straight lines depicted in gure 6 were obtained from a simultaneous linear t of the two sets of data points with eq.(6). The t yields the intersection of the lines with the energy axis, which according to eq.(6) will occur at the energies $h \;\; = E_0 = 1{:}581$ eV and

$h = E_0 + {}_e + {}_h = 1{:}604$ eV. The heavy-hole miniband energy width can be estimated theoretically from the solution of the Schroedinger-Poisson equations for the given structure, and we obtain ${}_h = 0{:}3$ meV, i.e. the hole dispersion can be ignored as a good approximation, hence we can deduce $E_0 = 1{:}581$ eV and ${}_e = 23$ meV. The latter parameter is in reasonable agreement with the electronic miniband width estimated from the Shubnikov-de Haas measurements, ${}_e = 19{:}6$ meV. The slope of the line determines the reduced effective mass of the electron-hole pair, i.e. $= 0{:}0612 m_0$. The estimated superlattice band gap, $E_0 = 1{:}581$ eV, can be compared to the theoretical value of the band gap, obtained from the $k \quad p$ equation for this structure, $E_0^{th} = 1{:}605$ eV, which does not take into account the lowering of the band gap due to many body effects. By equating $E_0 = E_0^{th} + BGR$, we obtain $BGR = \quad 24$ meV. For an electron gas confined in two dimensions, the band gap renormalization is[14] $BGR^{2D} = \quad 3{:}1 (na_X^2)^{1=3} E_X$ meV, where a_X and E_X are the exciton Bohr radius and binding energy, respectively, and $n = 1{:}42 \quad 10^{12}$ cm$^{\quad 2}$ is the areal density of electrons in the well. For a strictly two-dimensional electron gas, we substitute $E_X = 4R$, and an exciton radius of $a_X = a_B/2$, where R and a_B are the effective Rydberg and effective Bohr radius in bulk GaAs, respectively, to obtain $BGR^{2D} = 52$ meV. The finite thickness of the charges can be taken into account by calculating the exciton radius and binding energy for a 50A GaAs/$Al_{0{:}21}As_{0{:}79}As$ quantum well, as described in Refs[15,16], to give $E_X = 10{:}34$ meV and $a_X = 53$ A, in which case $BGR^{Q\,2D} = \quad 28$ meV. Finally, in the bulk the BGR is given by[17] $BGR = \quad 3{:}5 [n_{3D} (a_B)^3]^{1=4}$, where $n_{3D} = n/d$ is the equivalent bulk carrier concentration, which gives $BGR^{3D} = \quad 21{:}9$ meV. Thus, we find a BGR that is slightly larger than in the bulk, but is less than the BGR for a quasi two-dimensional system.

In conclusion, superlattice structures of GaAs/AlGaAs composition were produced, with a modulation doping profile that prevents the formation of Tamm states. Shubnikov-de Haas measurements in tilted fields demonstrate the presence of electrons confined by a superlattice potential in close agreement with the design parameters. PL was studied in high magnetic fields, and a broad luminescence band was observed above the GaAs band gap. For a fixed photon energy within this broad PL band, the intensity of the luminescence oscillates as a function of the magnetic field applied perpendicular to the superlattice layers. The PL oscillations are described by a doublet of frequencies, which show a linear dependence on the energy of the photon, showing that it is due to recombinations of electron-hole pairs confined by the superlattice potential. From the photoluminescence oscillations we can

estimate superlattice parameters – the electronic miniband width $_e$, the electron-hole pair reduced mass, , and the band gap renormalization, which we find is less than the BGR for a quantum well of the same barrier composition and well thickness, but greater than the BGR for a bulk GaAs degenerate electron gas.

IV. ACKNOWLEDGMENTS

This work was supported by FAPESP (Grants No. and 99/10359-7 and No. 01/00150-5) and CNPq (Grant No. 306335/88-3).

---

[1] M. Helm, W. Hilber, T. Fromherz, F.M. Peeters, K. Alavi and R.N. Pathak, Phys. Rev. B 48, 1601 (1993).

[2] H.T. Grahn, Semiconductor Superlattices – Growth and Eletronic Properties, (World Scientific, Singapore, 1995).

[3] R.H. Yan, R.J. Simes, H. Ribot, L.A. Coldren, and A.C. Gossard, Appl. Phys. Lett. 54, 1549 (1989).

[4] A.B. Henriques, R.F. Oliveira, P.L. Souza and B. Yavich, Physica B 298, 320 (2001); A.B. Henriques, Appl. Phys. Lett. 78, 691 (2001).

[5] M. Steslicka, R. Kucharczyk, A. Akjouj, B. Djafari-Rouhani, L. Dobrzynski and S.G. Davison, Surf. Sci. Rep. 47, 93 (2002).

[6] S. Schmitt-Rink, D.S. Chemla, and D.A.B. Miller, Adv. Phys. 38, 89 (1989).

[7] H.L. Stormer, J.P. Eisenstein, A.C. Gossard, W. Wiegmann, and K. Baldwin, Phys. Rev. Lett. 56, 85 (1986).

[8] Y. Iye, Materials science and engineering B – solid state materials for advanced technology, 31, 141 (1995).

[9] A.B. Henriques, L.K. Hanamoto, P.L. Souza, and B. Yavich, Phys. Rev. B 61, 13369 (2000).

[10] G. Bastard, Wave Mechanics Applied to Semiconductor Heterostructures, (Les Editions de Physique, Les Ulis, 1988).

[11] L.M. Roth, B. Lax, and S. Zwerdling, Phys. Rev. 114, 90 (1959).

[12] P. Voisin, G. Bastard, and M. Voos, Phys. Rev. B 29, 935 (1984).

[13] A. B. Henriques, Phys. Rev. B 50, 8658 (1994).

[14] S. Schmitt-Rink, c. Ell, S. W. Koch, H. E. Schmidt, and H. Haug, Sol. St. Commun. 52, 123 (1984).

[15] K. J. Moore, G. Duggan, K. Woodbridge, and C. Roberts, Phys. Rev. B 41, 1090 (1990).

[16] A. B. Henriques, Superl. Micr. 12, 527 (1992).

[17] T. L. Reinecke, and S. C. Ying, Phys. Rev. Lett. 43, 1054 (1979).

FIGURE CAPTIONS

Fig. 1 Fourier transform of the SdH oscillations for sample 2268, for a magnetic field applied normal to the surface of the sample. The labels indicate the saddle point in the density of states that originates a given frequency peak.

Fig. 2 Peak position of the Fourier transform of the SdH oscillations as a function of the angle between the magnetic field direction and the normal to the surface of the sample. The area of each dot is proportional to the intensity of the peak. The full and dashed lines correspond to the theoretical frequencies for the oscillatory components associated with saddle points M_0 and M_1, respectively.

Fig. 3 PL spectrum for the AlGaAs/GaAs superlattice. The superlattice band gap is indicated.

Fig. 4 PL intensity oscillations at fixed photon energies. The photon energy corresponding to each curve is shown.

Fig. 5 PL intensity oscillations at a photon energy of $h = 1.6199$ eV. Dots are the experimental values and the full line is a fit with equation (5). The best fit values of the adjusting parameters are shown.

Fig. 6 PL intensity oscillations at a photon energy of $h = 1.6199$ eV. Dots are the experimental values and the full line is a fit with equation (5). The best fit values of the adjusting parameters are shown.

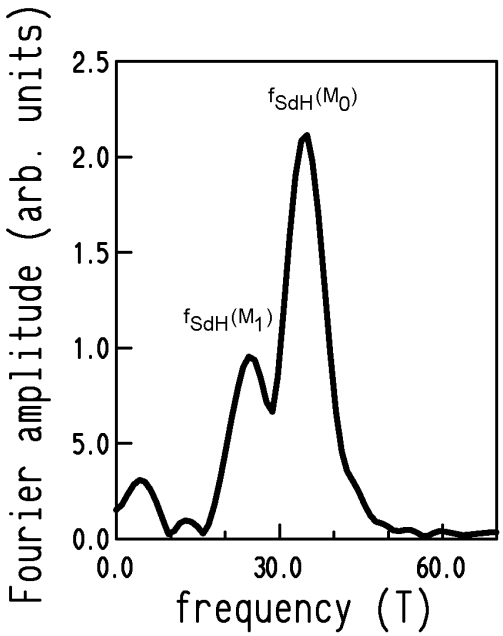

FIG.1:

Manuscript by Henriques et al, Figure 1

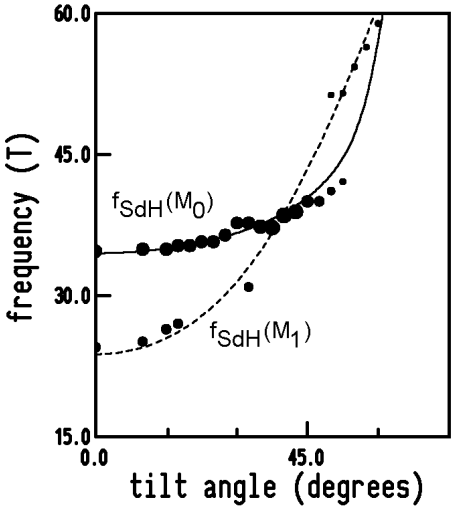

FIG.2:

Manuscript by Henriques et al, Figure 2

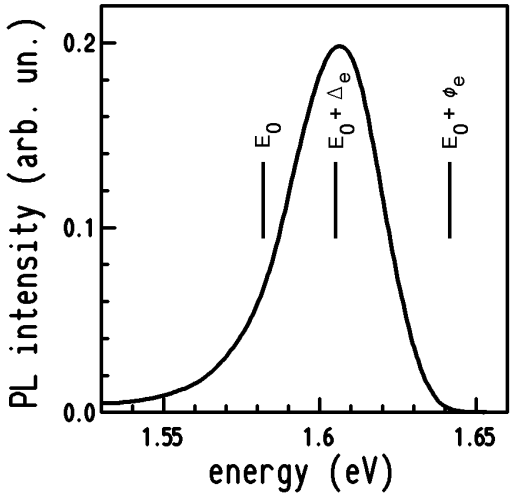

FIG. 3:

Manuscript by Henriques et al, Figure 3

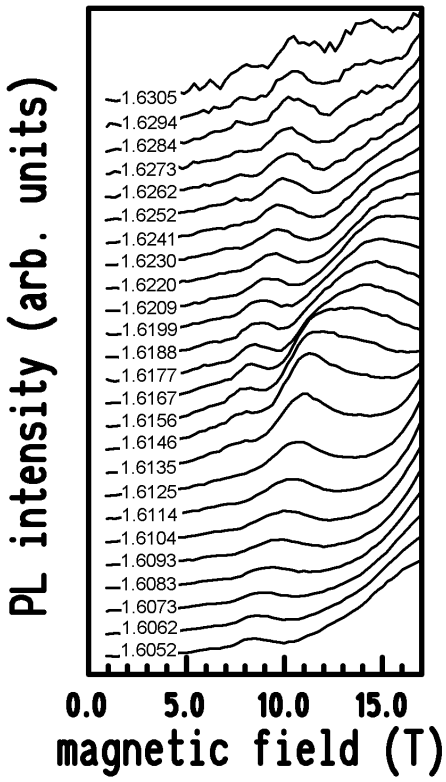

FIG. 4:

Manuscript by Henriques et al, Figure 4

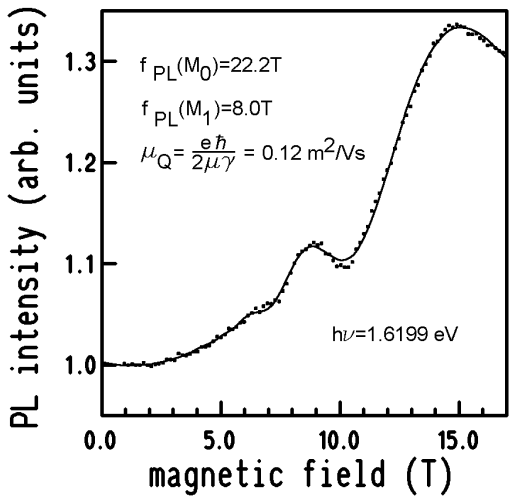

FIG. 5:

Manuscript by Henriques et al, Figure 5

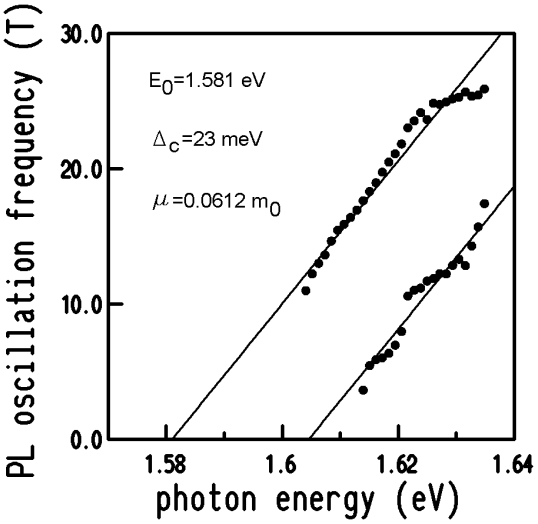

FIG. 6:

Manuscript by Henriques et al, Figure 6